EARTHQUAKE ENGINEERING AND STRUCTURAL DYNAMICS, VOL. 25, 319–332 (1996)

ESTIMATION OF SITE AMPLIFICATION FROM DAHAN DOWNHOLE RECORDINGS

HUEY-CHU HUANG AND HUNG-CHIE CHIU
Institute of Earth Sciences, Academia Sinica, P.O. Box 1-55, Nankang, Taipei, Taiwan, R.O.C.

SUMMARY

Four-level Dahan downhole recordings are used to investigate site amplification due to the near-surface structure. The downhole array is installed at the depths of 0 m (surface), 50, 100 and 200 m. Eight sets of data presenting well-separated incident and reflected waves (from the free surface) are selected to analyse the site amplification. Five techniques of spectral ratios have been tested to determine the most reliable way to estimate site response. The superior one is the ratio of Root-Mean-Square (RMS) Fourier amplitude spectra, because it has the minimum number of pseudopeaks. However, the pseudopeaks can be further reduced by omitting those ratios with small denominators. Results show that the amplification factors are nearly uniform at the depths of 50 and 100 m, where their values fall between one and two. This factor is frequency-dependent at the surface and in the range from two to five under 6 Hz. These results agree well with those from time-domain analyses and the transmission-coefficient estimation except that the latter overestimates the amplification factor of the surface station. This suggests that the shallow velocity structure provided by the geotechnical survey might be underestimated. Numerical modelling also supports the underestimation of velocity at near surface since the synthetic SH waves based on a modified velocity model can match these observations well.

KEY WORDS: site amplification; spectral ratio; waveform simulation

INTRODUCTION

The damage patterns of some recent earthquakes have shown that earthquake ground motion can be significantly amplified by near-surface sedimentary layers. Several well-known examples of the damage patterns were found in the 1985 Michoacan, Mexico earthquake, the 1988 Armenian earthquake, the 1989 Loma Prieta earthquake and the 1994 Northridge earthquake in California. Therefore, with the greatly enhanced level of damage that can be produced, it is quite important to develop methods for assessing the potential for, and the nature of, sediment amplification, especially when the location and the design of critical and essential facilities are being chosen. In this paper, the authors primarily focus the issue on site-specific amplification.

Site amplification is a complicated problem. A detailed discussion on the classification of site conditions, the estimation of amplification factors, analytical methods and numerical modelling for site response was given in Aki.[1] In that paper, emphasis was mainly placed on the site amplification of soil-to-rock sites and topographic effects. Besides these studies, downhole data are useful in the investigation of site amplification due to the near-surface structure. Borehole studies can directly estimate site response by providing a comparison of the response of surface material with that of the underlying bedrock. Joyner *et al.*[2] studied weak-motion data from a 186 m-deep downhole array on the shore of the San Francisco Bay where the ground motions were amplified at the surface by a factor of four or five. Hauksson *et al.*[3] analysed site response, Q values and f_{max} from a 1500 m-deep, three-level downhole array in the Los Angeles Basin. They found amplification factors of 4 for P waves and 9 for S waves. Seale and Archuleta[4] studied the site amplification and attenuation of strong ground motion from the McGee Creek 166 m-deep downhole in the Mammoth Lakes area of California where the peak accelerations at the surface were 5·7 times greater than those recorded at downholes. They considered that the major cause of amplification was attributed to the

CCC 0098–8847/96/040319–14

Received 21 March 1995
Revised 22 September 1995

resonance of the signal in the surface layers, and the amplification due to the resonance can compensate for the attenuation due to the low Q near the surface. Blakeslee and Malin[5] analysed stacked ratios of 157 microearthquake source spectra recorded at the surface and 200 m downhole at Parkfield, California, but did not find any systematic variation with azimuth or season. Archuleta *et al.*[6] analysed recordings from the Garner Valley downhole array in Southern California and found that deconvolving the complicated site effect from a surface recording was not always straightforward. This is because the S-wave time window includes not only the site effects for the S wave but also the site effects on the P-wave coda.

In general, site response can be estimated from different kinds of spectral ratio. In order to isolate the effects due to site conditions from those of the source or path, a common practice is to produce a spectral ratio by dividing the amplitude spectrum of the soil site by that of the rock site. In addition, the cross-spectrum ratio and response-spectrum ratio are often used to estimate site response, but the latter lacks definite physical meaning and the maximum response might not occur at the same time. In practice, Bendat and Piersol[7] explicitly encouraged the use of cross-spectrum ratios. This is because, in engineering applications, the input signals are generally well-known and are often specified explicitly, while the output signals contain a relatively greater level of noise. Safak[8] also suggested using the cross-spectrum estimate in favour of the spectral-ratio estimate to characterize site amplification. As regards the uncertainties and biases associated with various site response estimates, Field *et al.*[9] suggested that the spectral-ratio estimate is better than the cross-spectrum estimate if the input and output signals have equal levels of noise. If there is relatively less noise in the input signal than in the output, then the cross-spectrum estimate is better. In sediment site response studies, the spectral-ratio estimate[10–12] has been used almost exclusively. In fact, these two methods have both their benefits as well as shortcomings. The common defect between them is the spectral hole which produces a pseudopeak on the spectral ratio. Thus, how to overcome the effect from the spectral hole is an important problem.

One of the goals in this paper is to find an optimum estimate for site response. Here several tests are performed and a technique to overcome the spectral-hole problem is proposed. Furthermore, in order to find the optimum quantity to represent the site amplification of horizontal ground motion, the ratios of the EW, NS component, RMS, the complex signal and the maximum-polarization-direction signal of ground motion at surface and 200 m depth are compared. Eight earthquakes, whose records possess well-separated upgoing (or direct S) waves and downgoing (or reflected) waves at the depth of 200 m, are selected to analyse site amplification. Besides the analysis of site response in the frequency domain, the ratios of the peak ground acceleration (PGA), velocity (PGV), and displacement (PGD) in the time domain are used to check the amplification factor. In addition, based on the velocity structure, the transmission coefficients and the amplification factors with respect to each layer are also estimated. Finally, the Haskell method with a horizontal-layer model is used to simulate ground motion and verify the amplification factors.

DAHAN DOWNHOLE ARRAY AND DATA

The Dahan downhole array (represented by the square symbol in Figure 1) is located to the north of Hualien city in eastern Taiwan. Four triaxial downhole force-balance accelerometers (FBA-23D) were installed at the Dahan site in March 1992. Each channel of recordings is digitized with a 16-bit A/D converter at a sampling of 200 samples/sec. These instruments are at the depths of 0 m (surface), 50, 100 and 200 m within an area of 3 m × 3 m. A schematic cross-section of the site, the deployment of instruments, geology and the velocity profiles of the P and S waves are shown in Figure 2. Based on the site, gravel is a generic term in this site except for some alluviums at near surface 0·5 m. The orientation error of these downhole instruments was corrected by Chiu *et al.*[13] Figure 3(a) shows the corrected NS-component accelerograms recorded at the depths of 0, 50, 100 and 200 m at the Dahan site in the 8 August 1992 earthquake. The amplitudes gradually increase from 200 m depth to surface. The acceleration record is integrated into velocity and displacement. Figure 3(b) shows the NS-component displacement relevant to acceleration given in Figure 3(a). Evidently, the upgoing (or direct S) and downgoing (or reflected) waves appear on the 200 m-depth seismogram, where their corresponding times are about 12 and 12·8 sec, respectively. In this paper, site amplification due to the near-surface structure is examined, so only the upgoing wave was considered in the exclusion of multiple

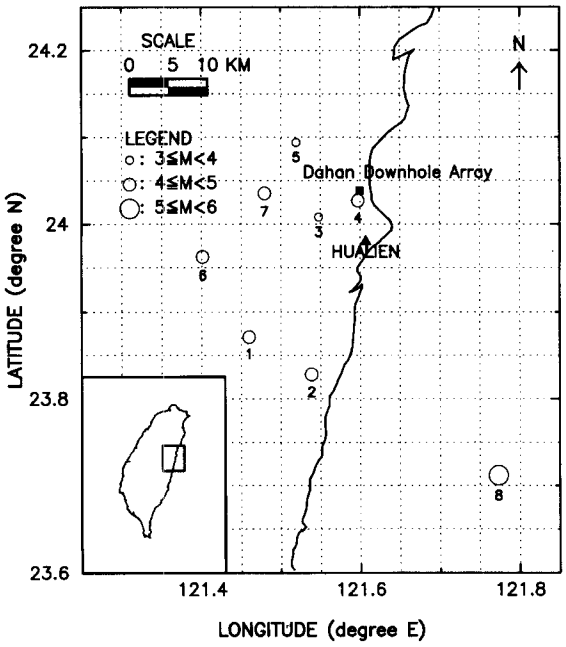

Figure 1. The site of the Dahan downhole accelerometer array, marked with a square symbol, is located in the Hualien area of Taiwan. Open circles represent the epicentres of the eight selected earthquakes

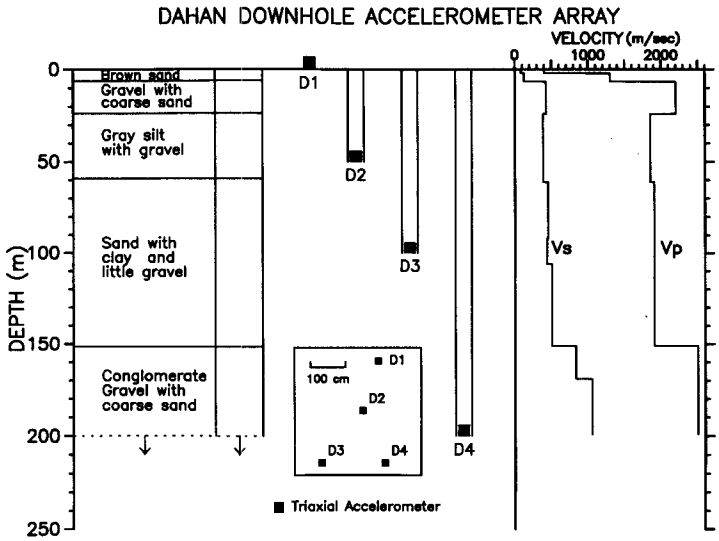

Figure 2. A schematic cross-section of the geology, site instrumentation and velocity profile are shown. Gravel is a generic term used in this site. Three-component downhole force-balance accelerometers (FBA-23D) were installed at the Dahan in March 1992 at the depths of 0, 50, 100 and 200 m

reflection. In order to do so, eight sets of data revealing well-separated incident and reflected waves (from the free surface) are selected in this study. Table I provides a list of these earthquakes and their source parameters. Only a 3-sec time-window length, primarily including the upgoing wave and the waves before it, is considered and cut by a 0·1-sec cosine taper. This treatment not only can prevent the confusion caused by

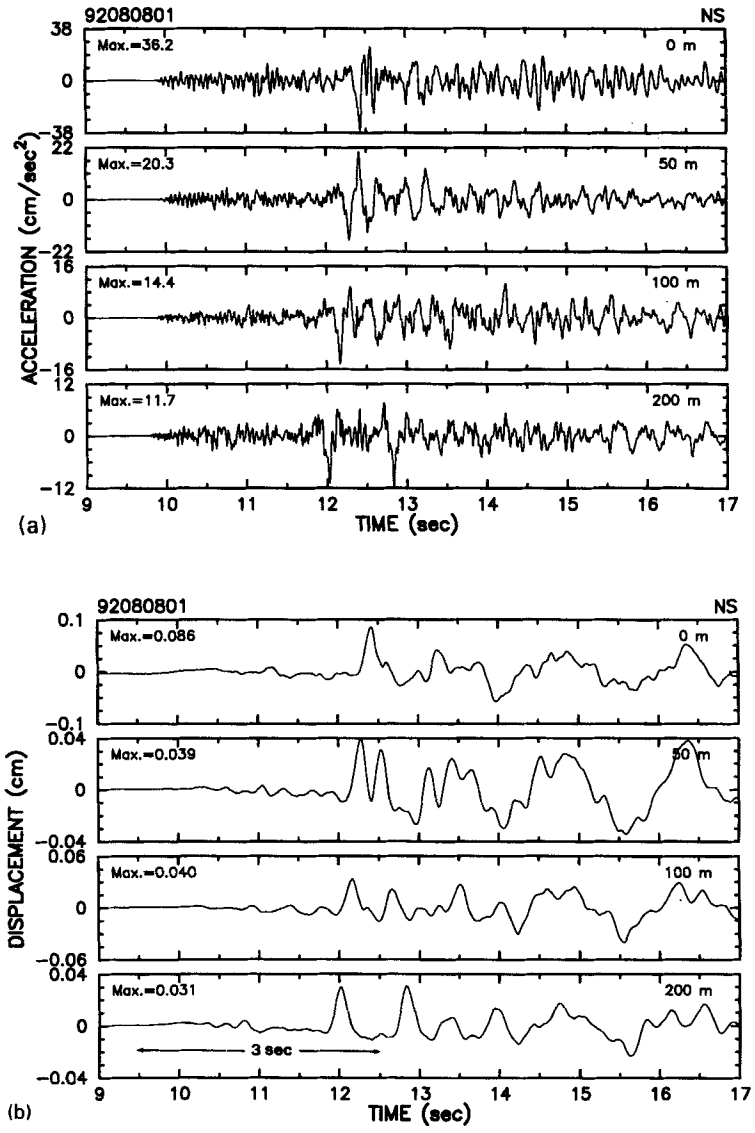

Figure 3. The NS-component seismograms of (a) acceleration and (b) displacement at the depths of 0, 50, 100 and 200 m for the 8 August 1992 earthquake. The upgoing and downgoing waves evidently appear in the seismograms (i.e. the times are about 12 and 12·8 sec at the depth of 200 m)

reflected waves, but also can increase the Fourier-transform resolution better than that by only choosing the upgoing wave.

EMPIRICAL SITE-RESPONSE ESTIMATE

Methods

The conventional method used to estimate the site response is the Fourier spectral ratio[14, 15], $S_{sr}(f)$. The ratio between $F_1(f)$ at the soil site and $F_2(f)$ at the reference site can be expressed as

$$S_{sr}(f) = F_1(f)/F_2(f) \tag{1}$$

Table I. The source parameters of eight used earthquakes

No.	Earthquake series No.	Latitude (degree)	Longitude (degree)	ML	Δ (Km)	Depth (Km)	θ (degree)
1	92053101	23·87	121·46	4·5	23·5	12·6	219·0
2	92060101	23·83	121·54	4·4	24·2	4·6	195·5
3	92060801	24·01	121·55	3·8	6·5	18·0	238·4
4	92062501	24·03	121·60	4·8	1·4	22·7	200·9
5	92062502	24·09	121·52	3·8	10·4	13·4	306·1
6	92072301	23·96	121·40	4·8	22·1	12·8	247·4
7	92080801	24·03	121·49	4·6	12·0	12·7	267·5
8	92090101	23·71	121·77	5·2	40·2	51·4	154·3

Note: Δ: epicentral distance, θ back-azimuth.

To estimate amplification factors, the cross-spectrum method[8, 16] can be represented in the following form:

$$S_{cr}(f) = S_{12}(f)/S_{11}(f) \tag{2}$$

where $S_{cr}(f)$ is the frequency response function between reference sites 1 and 2; $S_{12}(f)$ is the cross-spectrum of records at sites 1 and 2 ($A_1(t)$ and $A_2(t)$); and $S_{11}(f)$ is the power spectrum of $A_1(t)$.

In general, the site response is usually estimated from a single-component record. This, however, does not present the characteristics of ground motion well because the orientation of the instrument is arbitrary and independent of the back-azimuth of an earthquake. In order to obtain a good representation of the horizontal ground motions, Lu *et al.*[16] and Tumarkin and Archuleta[17] proposed a complex signal to treat both horizontal time histories as a two-dimensional signal by forming a complex time-series:

$$A_c(t) = A_x(t) + \mathrm{i}\, A_y(t), \tag{3}$$

where $A_c(t)$ represents the total amplitude of horizontal ground motions ($A_x(t)$, $A_y(t)$). Although this method does not consider the two horizontal spectra individually, rotate the axes or take the RMS of the two spectra, the physical meaning of $A_c(t)$ is not very clear. The applicability of the complex signal is discussed in the next section. Chiu and Huang[18] suggested that the RMS ratio could be a good estimator and that it represents the maximum value of the two horizontal spectra.

Optimum site-response estimate

To find a good site-response estimate is necessary in the calculation of site amplification. Two important factors, background noise and spectral hole, should be considered in calculating the spectral ratio. Therefore, before estimating the site response, the level of background noise at the Dahan site needs to be investigated. Figure 4 shows the comparison of the horizontal RMS spectrum between eight selected earthquakes (thick lines) and six microtremors (thin lines) at the depths of 0 and 200 m. The Fourier amplitude of earthquakes at the surface and at the depth of 200 m are 0·2–20 cm/sec and 0·1–10 cm/sec, whereas the Fourier amplitude of microtremors at the surface and at the depth of 200 m are 0·005–0·05 cm/sec and 0·001–0·005 cm/sec, respectively. Obviously, the background noise at the depth of 200 m is smaller than that at the surface site. Therefore, the station at the depth of 200 m is selected as the reference site in estimating site response. Since the amplitudes of earthquakes are much larger than those of microtremors, the effect coming from background noise is negligible. In fact, the major factor that can affect the spectral ratio is the presence of pseudopeaks due to spectral holes. In order to solve this problem, a criterion is selected so as to omit some ratios when their denominators are less than a given value. However, the criterion is determined by the level of microtremors. Figure 5 shows the average of the Fourier spectrum for six records of microtremors at the depth of 200 m, where the plots from top to bottom represent the root mean square (RMS), NS, vertical and EW components. The RMS values are the combinations of the NS- and EW-component spectra. To compare

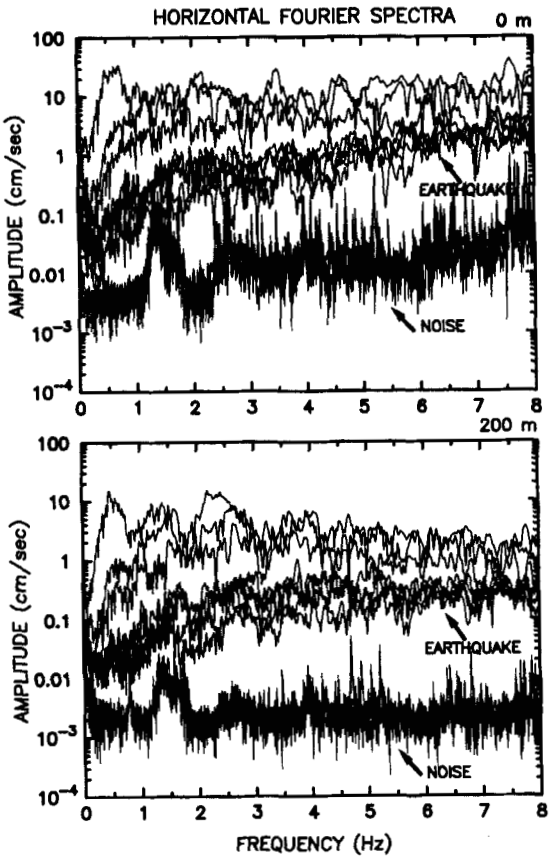

Figure 4. The comparison of the horizontal RMS spectra among eight selected earthquakes (thick lines) and 6 microtremors (thin lines) at the depths of 0 and 200 m

these spectra, most of the amplitudes are under 0·01 cm/sec. Therefore, the criterion is set to 0·1 cm/sec which is ten times that of the peak value. The modification can effectively reduce the number of pseudopeaks; nevertheless, some other normal ratios have been omitted.

In this paper, Fourier spectra are calculated without any smoothing operator being applied. Figure 6(a) shows the original spectral ratios, where the Fourier spectrum of surface record is divided by that of the reference site. In order to find the optimum quantity to represent the horizontal ground motion, the authors compare the spectral ratios of the NS, EW component, the complex signal (CMPLX), the maximum-polarization-direction signal (Max. Polar.) and the RMS signals for eight selected earthquakes. The eight different symbols represent ratios coming from the eight different earthquakes, while the solid lines represent their averages. In the plots of ratios, the pseudopeaks or anomalous peaks appear in all cases except in the RMS component. This points out the unstable results due to the spectral hole. The main source of these pseudopeaks is the use of small denominators. After some points are omitted, the results are shown in Figure 6(b). Omitting points has effectively removed most pseudopeaks, although a few still do exist in the NS, EW and CMPLX (complex) signals. Besides the unstable character, the single (NS or EW) component is not significant enough to describe horizontal ground motion because the orientation of the instrument is independent of the back-azimuth of an earthquake. Although the complex signal combines two horizontal components, the spectral-hole problem is still present. In addition, the complex signal can exaggerate the peak and the trough of the spectrum, thereby inducing some pseudopeaks when the ratio is calculated. And what is more, the physical meaning of this complex signal is not very clear; hence this is not used in the study. The spectral ratios in the maximum polarization direction have results similar to those of the RMS ratios.

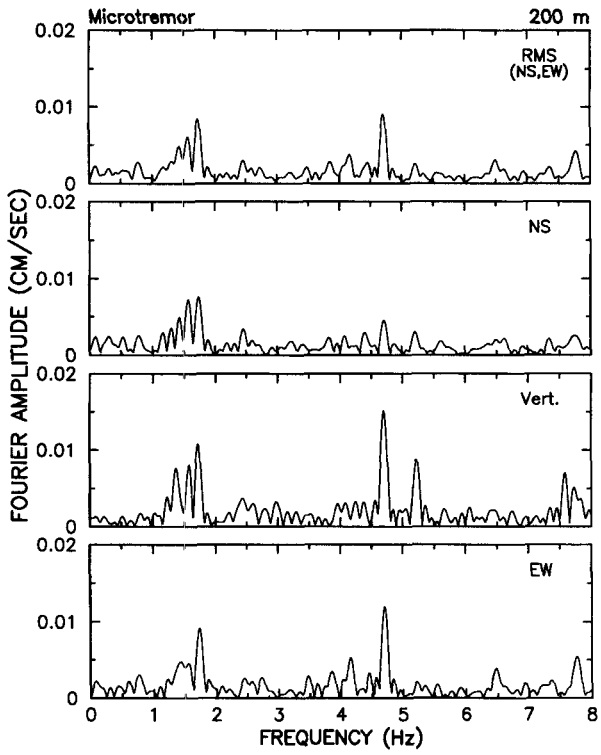

Figure 5. The average of the Fourier spectra for six microtremors at the depth of 200 m, where the plots from top to bottom represent the RMS, NS, vertical and EW components. The maximum value of amplitude is under 0·01 cm/sec

For comparison, the data at downholes should be rotated in the same direction. However, the maximum polarization directions at different depths are not always the same. Therefore, this polarized signal is not used in this study. In summary, the RMS signals might be the most reliable one to represent horizontal ground motions.

SITE AMPLIFICATION ANALYSIS

Spectral ratio

Fourier-spectrum and cross-spectrum estimates bear similar results except at spectral holes at some frequencies. In this paper, only the results of the Fourier-spectrum ratio are presented. This ratio represents the amplification factor for direct-S waves and does not include site resonance. In this paper, the 200 m-depth station is chosen as the reference site.

Figure 7 shows the mean Fourier-spectrum ratio of eight selected events for the RMS component at the depths of 0, 50 and 100 m corresponding to the reference site. The ratios are after omitting-point process, while the criterion is set to 0·1 cm/sec. Only the results under 8 Hz are discussed in this paper because above this, the signals are weak. The ratios at the 50 m-depth site are similar to those at the 100 m-depth site and are almost independent of the frequency, being close to two. However at surface site, the amplification factors are frequency dependent, being 2–3 under 3·3 Hz, 3–4 between 3·3 and 5 Hz, 4–5 between 5 and 6 Hz. The large amplification factor and variance in surface records can be interpreted as the results of scattering effect because these high-frequency signals do not appear in downhole records.

PGA, PGV, PGD ratios

In order to examine the amplification factor in the time domain, the authors have studied the ratios of Peak Ground Acceleration (PGA), Velocity (PGV) and Displacement (PGD) at the depths of 0, 50 and 100 m

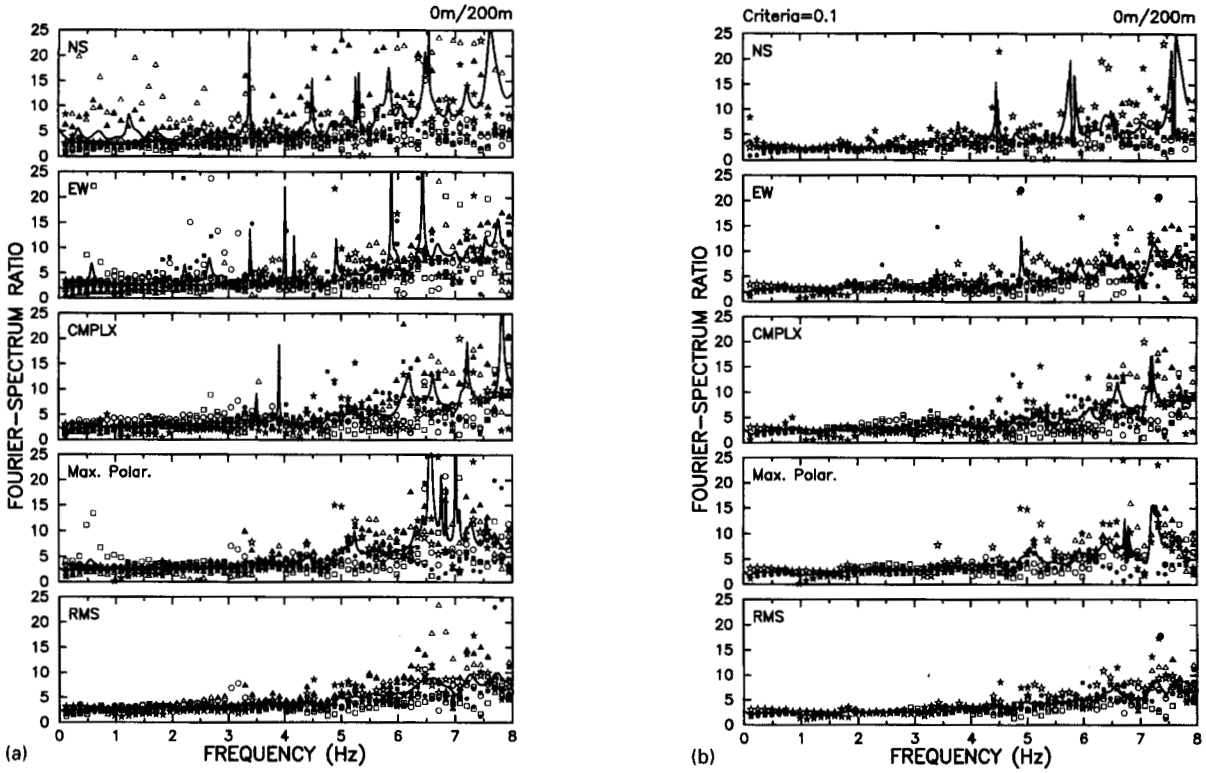

Figure 6. The spectral ratios of the NS-, EW-components, RMS, the complex signal and the maximum-polarization-direction signal of ground motions (0 vs. 200 m) represent the site amplifications of different horizontal ground motions for eight selected earthquakes. The different symbols represent ratios coming from different earthquakes while the solid lines indicate their average: (a) in the original, (b) after omitting point

corresponding to those at the depth of 200 m. The selection of the time window is the same as that in the calculation of the spectral ratios. Figures 8(a)–8(c) show these results. The PGA, PGV and PGD ratios of the NS component (triangle symbols) are similar to those of the EW component (circle symbols) at the depths of 50 and 100 m. The means of these components are listed in the upper-left corner of each plot. Their values at the depths of 0, 50 and 100 m are about 4·4, 1·7 and 1·6 for PGA ratios, but about 3·5, 1·6 and 1·3 for PGV and PGD ratios. Evidently, the PGA ratios, representing the high-frequency ratio, are higher than the PGV and PGD ratios at the surface site. These results are in good agreement with the spectral ratios in the frequency domain (Figure 7).

Transmission coefficient

The transmission coefficients[19] are also calculated to check the site amplification at the Dahan site. The transmission at the interface of the ith layer and $(i + 1)$th layer should be considered next. When the unit impulse is incident from the $(i + 1)$th layer, the researchers designated the transmitted impulses as t_i, and obtain the relation

$$t_i = \frac{2\rho_{i+1}C_{i+1}}{\rho_{i+1}C_{i+1} + \rho_i C_i} \tag{4}$$

The P- and S-wave velocity structures (Figure 2) and bulk density distribution of 10 layers were provided by seismic survey.[20] The corresponding values are listed in Table II. From these, transmission coefficients and amplification factors in each layer are calculated. The amplification factors at the depths of 0, 50 and 100 m are

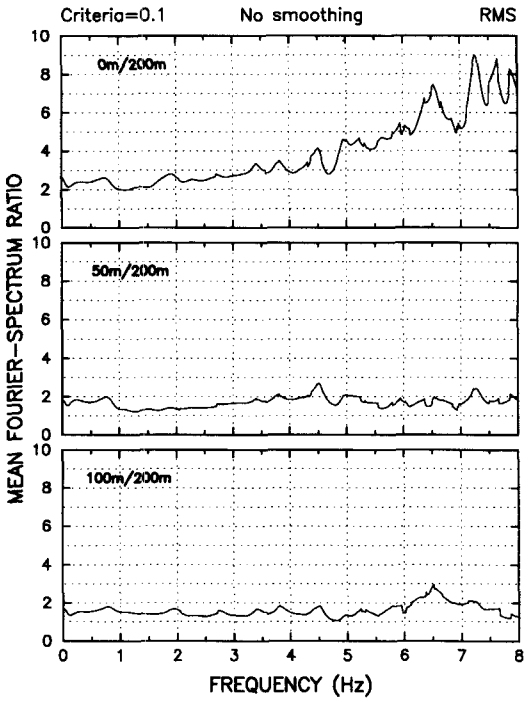

Figure 7. The mean Fourier-spectrum ratios of eight chosen events for the RMS component at the depths of 0, 50 and 100 m corresponding to the reference site. The ratios are after omitting-point process, while the criterion is set to 0·1 cm/sec

Table II. Velocity structure and amplification factor at the Danhan array

Layer No.	Depth (m)	Vs (m/sec)	Density (g/cm^2)	Transmission coefficient	Amplification factor
1	0·0	0	0·00	2·0	5·7
2	2·0	80	2·10	1·2	2·8
3	6·5	125	2·09	1·5	2·3
4	24·0	428	2·04	0·9	1·5
5	61·0	385	2·05	1·1	1·6
6	92·0	454	2·07	1·0	1·5
7	106·0	438	2·07	1·1	1·5
8	151·0	500	2·08	1·2	1·4
9	169·0	833	2·08	1·1	1·1
10	200·0	1050	2·09	1·0	1·0

about 5·7, 1·6 and 1·5, respectively. The amplification factors at the depths of 50 and 100 m are reasonable, but that at the surface site is higher than the values estimated under the previous two methods. The most likely reason for this is the underestimation of the surficial velocity. This question is verified somewhat from the numerical modelling.

Numerical modelling

The Haskell method[21, 22] is used to calculate the site amplification of the horizontal and layered structure at the Dahan site. The ground motion at the surface site is chosen as the input to predict the ground motion

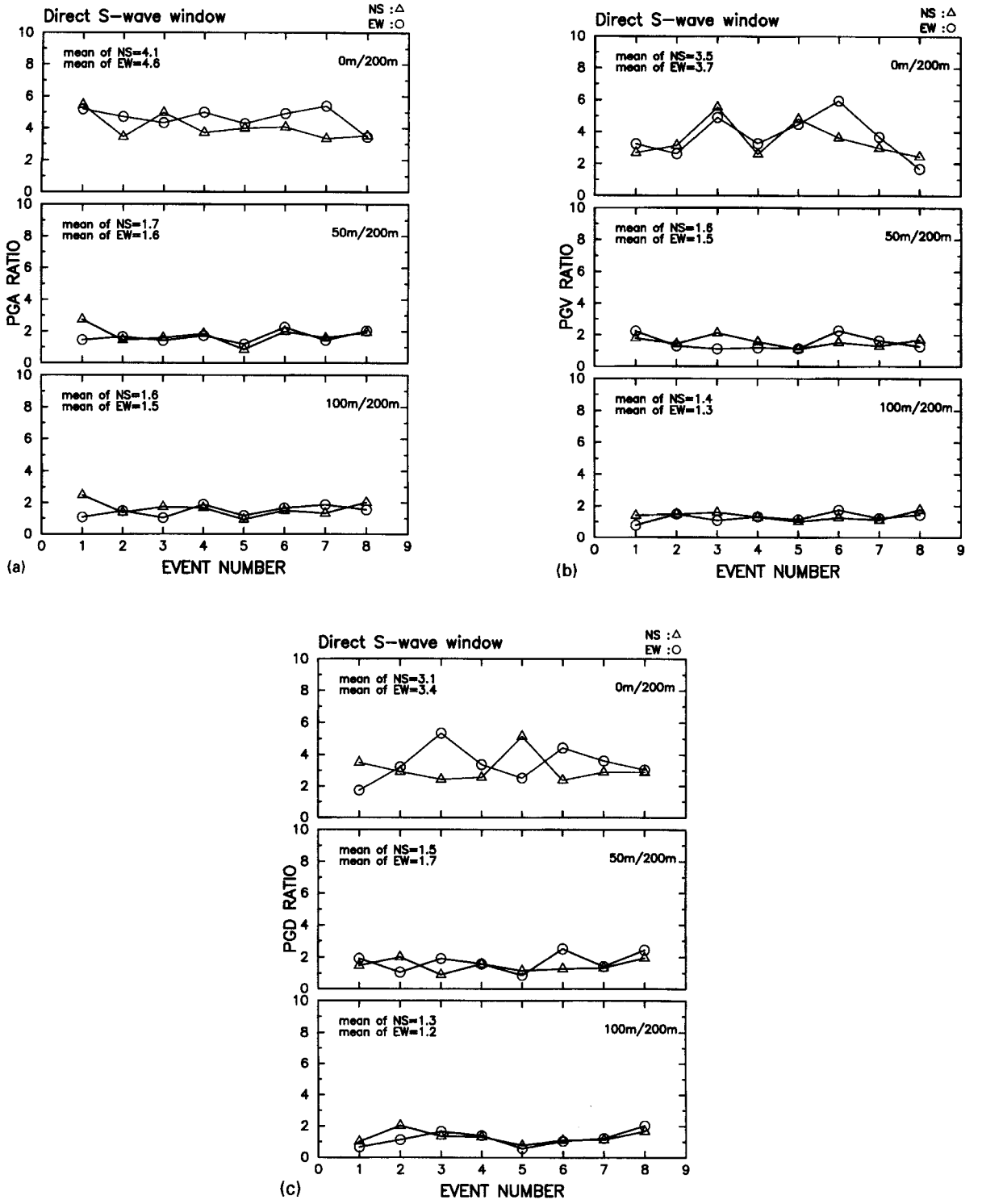

Figure 8. The PGA-, PGV- and PGD-ratio distributions for the same eight events. Three plots from top to bottom represent depths of 0/200 m, 5/200 m and 100/200 m, where (a)–(c) are for the PGA-, PGV- and PGD-ratio distributions

Table III. Velocity structure at the Danhan downhole array

Layer No.	Depth (m)	Vp (m/sec)	Vs (m/sec)	Vs* (m/sec)	Density (g/cm^3)	Density* (g/cm^3)
1	0–2	400	80	133	2·10	2·00
2	2–6·5	1300	125	231	2·09	2·01
3	6·5–24	2200	428	398	2·04	2·04
4	24–50	1850	385	398	2·05	2·05
5	50–61	1850	385	398	2·05	2·05
6	61–92	1905	454	454	2·07	2·07
7	92–100	1905	438	438	2·07	2·07
8	100–106	1905	438	438	2·07	2·07
9	106–151	1905	500	500	2·08	2·08
10	151–169	2500	833	833	2·08	2·08
11	169–200	2500	1050	1050	2·09	2·09
12	200–	2500	1050	1050	2·09	2·09

*Represents the modified velocity structure.

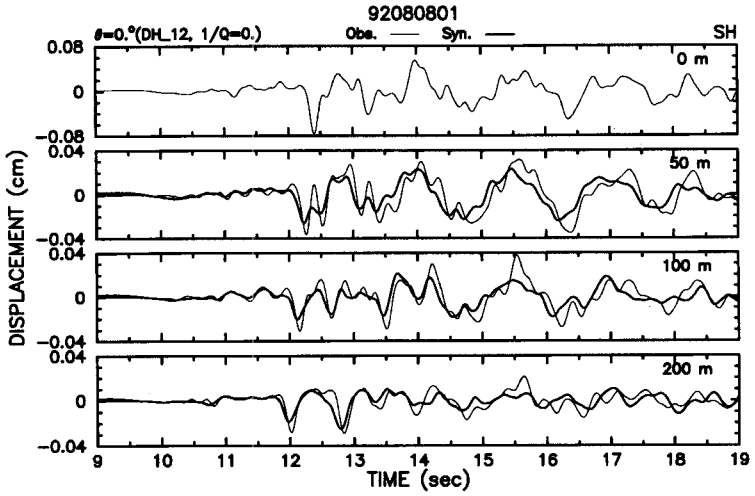

Figure 9. The synthetic results (thick lines) are compared with the observed data (thin lines) for the velocity structures provided by seismic survey and listed in Table II. The SH wave is vertically incident from the half-space (200 m). The surface ground motion is used to predict those at the other depths

at the depths of 50, 100 and 200 m. The great advantage of this approach is that the upgoing (or direct S) wave need not be separated from the downgoing (or reflected) wave. By means of this technique, the whole waveform corresponding to each layer can be calculated directly. The used velocity structure and density are listed in Table III. No attenuation term ($1/Q_s = 0$) is added to the simulating process. This is because the effects of Q_s values are small; it is assumed to be negligible here.

In this part, the recordings of the 8 August 1992 earthquake at the Dahan site are analysed. According to the back-azimuth (267·5°) of this earthquake, two horizontal components are used to construct the SH wave. The velocity structure is divided into 10 layers and is considered to be at the half-space under the 200 m depth. It is assumed that the SH wave is vertically incident from the half-space and the ground motion at surface site is used to predict motion at downholes. Figure 9 shows the synthetic results (thick lines) compared with the observed data (thin lines). However the synthetic S wave (11·7–13 sec) matches the observed one neither in amplitude nor in phase. This indicates that there are some problems in the velocity

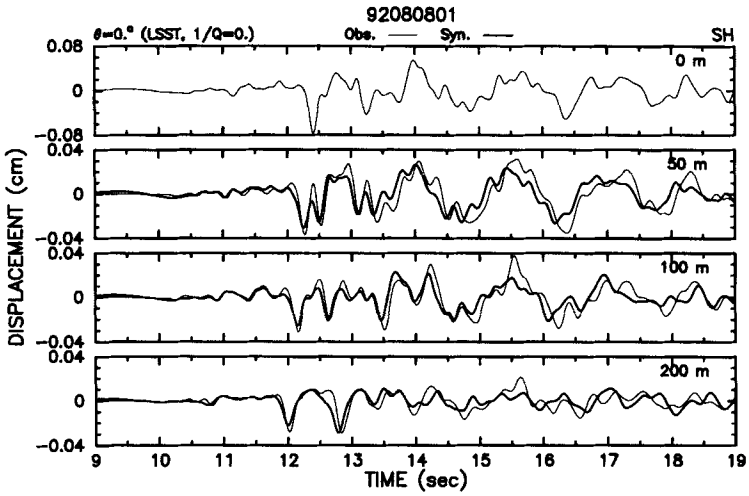

Figure 10. The synthetic results (thick lines) are compared with the observed data (thin lines) for the corrected velocity structures listed in Table III (marked by *)

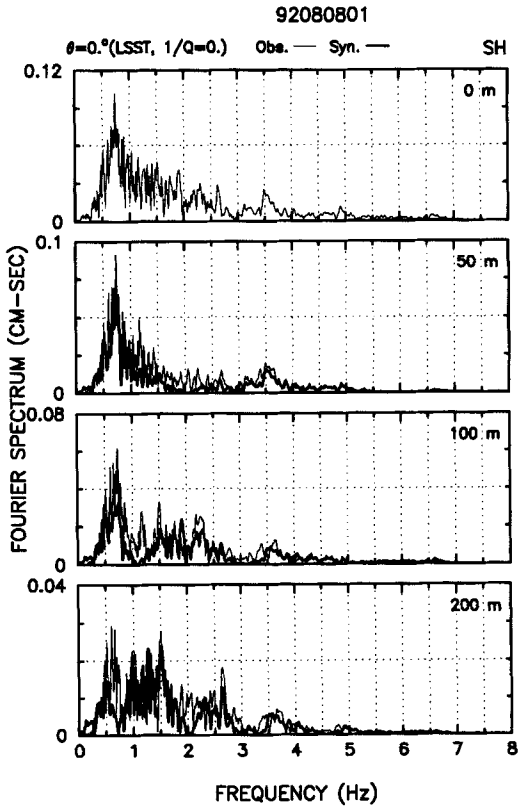

Figure 11. The synthetic Fourier spectra (thick lines), based on the Haskell method, compared with the observed Fourier spectra (thin lines)

structure. However, according to the discussion in the previous section, it also indicates that the velocity at shallow depths needs to be examined more thoroughly. Therefore, a modified S-wave velocity structure is constructed and corresponding values are listed in Table III (marked by *). Figure 10 shows the synthetic waveforms for the corrected velocity structures. Evidently, although the reflected wave arrives later, the

phase of upgoing wave fits better. The results cannot be improved by means of adjusting velocity or incident angles. Figure 11 shows the synthetic Fourier spectra (thick lines), based on the Haskell method, compared with the observed Fourier spectra (thin lines). Most synthetic spectra at the depths of 50, 100 and 200 m compare well with the observed ones. However, amplitudes at predominant frequencies are underestimated. In general, the modified model gives a better simulation of ground motions.

CONCLUSIONS

The four-level Dahan downhole recordings at the depths of 0, 50, 100 and 200 m are used to investigate site amplification due to the near-surface structure. It is shown that the best spectral method to estimate this amplification is the ratio of the root-mean-square Fourier amplitude spectra between the given site and the reference site (selected at 200 m depth). It should be noted that the pseudopeak due to a spectral hole presents a serious problem in the spectral ratio. However, these pseudopeaks can be removed effectively by omitting those ratios which come from small denominators. Eight earthquakes, in which the upgoing (or direct S wave) and downgoing (or first reflected wave) phases at the 200 m depth are well-separated, are selected to analyse the site response. The amplification factors at the depths of 50 and 100 m fall between one and two. This factor is frequency dependent at the surface in a range 2–5 under 6 Hz, whereas it is 2–3 under 3·3 Hz, 3–4 between 3·3 and 5 Hz, and 4–5 between 5 and 6 Hz. These results in the frequency domain are consistent with those of both time-domain and transmission-coefficient analyses, except that the surficial velocities are underestimated. Numerical modelling also shows this underestimation. In contrast, the modified model in this study provides a satisfactory prediction of the SH-wave amplification at the Dahan site.

ACKNOWLEDGEMENTS

The authors are grateful to Professor G. B. Warburton and three anonymous reviewers for their valuable comments. This research was supported by Academia Sinica and the National Science Council under contract NSC-83-P-001-001B. The support of these organizations is gratefully acknowledged.

REFERENCES

1. K. Aki, 'Local site effects on strong ground motion', in J. L. Von Thum (ed.) *Geotechnical Special Publication No. 20*, ASCE, New York, 1988, pp. 103–155.
2. W. B. Joyner, R. E. Warrick and A. A. Oliver, 'Analysis of seismograms from a down-hole array in sediments near San Francisco Bay', *Bull. seism. soc. Am.* **66**, 937–958 (1976).
3. E. Hauksson, T. L. Teng and T. L. Henyey, 'Results from a 1500 m deep, three-level downhole seismometer array: site response, low Q values, and f_{max}', *Bull. seism. soc. Am.* **77**, 1883–1904 (1987).
4. S. H. Seale and R. J. Archuleta, 'Site amplification and attenuation of strong ground motion', *Bull. seism. soc. Am.* **79**, 1673–1696 (1989).
5. S. Blakeslee and P. Malin, 'High-frequency site effects at two Parkfield downhole and surface stations', *Bull. seism. soc. Am.* **81**, 332–345 (1991).
6. R. J. Archuleta, S. H. Seale, P. V. Sangas, L. M. Baker and S. T. Swain, 'Garner Valley downhole array of accelerometers: instrumentation and preliminary data analysis', *Bull. seism. soc. Am.* **82**, 1592–1621 (1992).
7. J. S. Bendat and A. G. Piersol, *Engineering Applications of Correlation and Spectral Analysis*, Wiley, New York, 1980.
8. E. Safak, 'Problems with using spectral ratios to estimate site amplification', *Proc. 4th int. conf. seis. zonation* **2**, 1991, pp. 277–284.
9. E. H. Field, K. H. Jacob and S. E. Hough, 'Earthquake site response estimation: a weak-motion case study', *Bull. seism. soc. Am.* **82**, 2283–2307 (1992).
10. S. K. Singh, J. Lermo, T. Dominguez, M. Ordaz, J. M. Espinosa, E. Mena and R. Quass, 'The Mexico earthquake of September 19, 1985: a study of amplification of seismic waves in the Valley of Mexico with respect to a hill zone site', *Earthquake spectra* **4**, 653–673 (1988).
11. S. K. Singh, E. Mena and R. Castro, 'Some aspects of the source characteristics and the ground motion amplifications in and near Mexico City from the acceleration data of the September, 1985, Michoacan, Mexico earthquakes', *Bull. seism. soc. Am.* **78**, 451–477 (1988).
12. S. Midorikawa, 'A statistical analysis of submitted predictions for the Ashigara Valley blind prediction test', *Proc. int. symp. effects of surface geol. on seism. motion* **2**, 1992, pp. 65–80.
13. H. C. Chiu, H. C. Huang, C. L. Leu and S. D. Ni, 'Application of polarization analysis in correcting the orientation error of downhole seismometers', *Earthquake eng. struct. dyn.* **23**, 1069–1078 (1994).
14. C. Gutierrez and S. K. Singh, 'A site effect study in Acapulco, Guerrero, Mexico: comparison of results from strong-motion and microtremor data', *Bull. seism. soc. Am.* **82**, 642–659 (1992).

15. R. B. Darragh and A. F. Shakal, 'The site response of two rock and soil station pairs to strong and weak ground motion', *Bull. seism. soc. Am.* **81**, 1885–1899 (1991).
16. L. Lu, T. Katayama and F. Yamazaki, 'Soil amplification based on seismometer array and microtremor observations in Chiba, Japan', *Earthquake eng. struct. dyn.* **21**, 95–108 (1992).
17. A. G. Tumarkin and R. J. Archuleta, 'Parametric models of spectra for ground motion prediction', *Seism. res. lett.* **63**, 30 (1992).
18. H. C. Chiu and H. C. Huang, 'Azimuth-dependent site amplification', *TAO* **3**, 21–37 (1992).
19. K. Aki and P. G. Richard, *Quantitative Seismology Theory and Methods*, W. H. Freeman, San Francisco, 1980.
20. Chung-Chi Consultant Co. Ltd., Investigation report of drilling engineering for the downhole strong-motion seismometer arrays at the Jun-Kung Marble Plant and the Dahan Industrial School in Hualien, 1991 (in Chinese).
21. N. A. Haskell, 'The dispersion of surface waves on multilayered media', *Bull. seism. soc. Am.* **43**, 17–35 (1953).
22. N. A. Haskell, 'Crustal reflection of plane SH waves', *J. geophys. res.* **65**, 4147–4150 (1960).